CHINESE OPTICS LETTERS

Vol. 20, No. 10 | October 2022

Large bandgap oscillations in two-dimensional Dion–Jacobson phase perovskites caused by coherent longitudinal acoustic phonons [Invited]

Fengke Sun (孙逢柯), Boning Wu (吴博宁)*, and Shengye Jin (金盛烨)**

Dalian Institute of Chemical Physics, Chinese Academy of Sciences, Dalian 116023, China

*Corresponding author: boning@dicp.ac.cn

**Corresponding author: sjin@dicp.ac.cn

Received August 19, 2022 | Accepted September 8, 2022 | Posted Online October 12, 2022

Two-dimensional Dion–Jacobson (D-J) phase perovskites are prospective photovoltaic and optoelectronic materials. To study their mechanical properties and carrier-lattice interactions, we conduct femtosecond spectroscopic experiments on the films of a D-J perovskite. After optical excitation, a ∼33 meV bandgap oscillation is observed in the film by transient absorption spectroscopy. With the help of transient reflection methods, we reveal that the oscillation originates from the transport of coherent longitudinal acoustic phonons through the film. Large bandgap oscillation indicates a strong coupling between carriers and lattice, and significant bandgap modulation by strains in D-J perovskites.

Keywords: transient absorption; coherent longitudinal acoustic phonons; bandgap oscillation; 2D Dion–Jacobson phase perovskites.

DOI: 10.3788/COL202220.100010

1. Introduction

Organic-inorganic hybrid metal halide perovskites are a group of fast-developing materials for photovoltaic and optoelectronic applications[1–4]. Compared to their three-dimensional (3D) analogs, two-dimensional (2D) perovskites exhibit many advantages, including large exciton binding energy[5–7], improved moisture resistance[8–10], and the tunability of the bandgap by adjusting the layer thickness[11–13].

The biggest family of 2D perovskites is the Ruddlesden–Popper (R-P) phase. In their structure, two adjacent −2 charged inorganic layers are separated by an interdigitating bilayer of two organic cations. Another type, Dion–Jacobson (D-J) phase perovskites, has been reported in recent years[14]. They have +2 charge spacer cations between two adjacent layers[15]. Therefore, the distances between inorganic layers in D-J phase perovskites are substantially shortened[16]. As a result, they exhibit different mechanical properties than the R-P phase, leading to the unique acoustic phonon behaviors and carrier-phonon interactions in them, which we attempt to study in this work.

We employ transient absorption (TA) and reflection (TR) experiments on the thin films of a 2D D-J phase perovskite, (DMAPA)PbI_4 [DMAPA represents 3-(dimethylammonium)-1-propylammonium]. In TA experiments, a bandgap oscillation of large amplitude (∼33 meV) and long period (tens to hundreds of picoseconds) is observed. By studying the dependence of oscillation on film thickness and excitation energy, we conclude that the oscillation originates from the transport of coherent longitudinal acoustic phonons (CLAPs) across the perovskite film. TR experiments verify the presence of the CLAP and measures the time that the CLAP travels through the film.

Previously, bandgap oscillation induced by the optical excitation method has been observed in perovskites, which could be explained by local oscillation of lattices caused by optical phonons[17,18] or coherent interactions between light field and matter (the optical Stark effect)[19–21]. These are all short-time interactions, leading to fast bandgap oscillations on a picosecond scale. In this work, since the cause of oscillation is the longitudinal transport of acoustic phonons across the film, it displays a larger amplitude and a substantially longer period than previously reported.

2. Experiments

2D perovskite (DMAPA)PbI_4 films were fabricated by a hot-casting spin-coating method reported previously[22]. To make a ∼286 nm thick film, a precursor solution was made by dissolving 90 mg (DMAPA)I_2 and 115 mg PbI_2 in 1 mL DMF and then stirred at 90°C for 2 h. Substrate glass slides were cleaned by sonication in water, ethanol, and acetone, respectively, before being

treated with oxygen plasma for 20 min. Clean substrate was preheated at 90°C for 5 min and then transferred onto a spin coater. 50 μL perovskite precursor solution was dropped on the substrate, followed by a spin-coating at 4000 r/min and 90°C for 20 s. Then, in an annealing process, the substrate was transferred to a 120°C hot plate and kept there for 5 min. Control of film thickness was achieved by adjusting the precursor solution concentration.

Femtosecond TA/TR is based on a setup described previously[23]. Amplified 800 nm laser pulses are generated by a Coherent Astrella, which contains an oscillator and a Ti:sapphire regenerative amplifier. The output laser pulses have 1 kHz repetitive rate, ~35 fs FWHM, and ~6 mJ of energy each. A beam splitter divides the laser, with one beam sent to a Coherent TOPAS optical parametric amplifier (OPA), generating the pump beam. The other beam is attenuated and focused on a CaF_2 crystal, creating a 350–800 nm white-light continuum used as the probe beam. The chirp of the probe pulse over time is less than 300 fs, as evaluated by looking at the nonresonance signal on the glass substrate. The pump and probe lights are focused and overlapped on the sample, and the transmitted/reflected probe beam was collimated and then collected by a fiber-coupled spectrometer with arrayed CMOS sensors. The time delay between pump and probe pulse was controlled by a motorized delay stage. The pump beam was chopped by a synchronized optical chopper at 500 Hz, and the change in absorbance or reflectivity (ΔA or $\Delta R/R$) was calculated by subtracting the intensity of two adjacent probe pulses (pumped and unpumped).

TA: Both pump and probe beams are incident on the sample from the perovskite–air interface. The probe beam transmits through the perovskite and substrate before collected by the detector. The probe incident angle is near normal, and the pump beam incident angle is slightly larger than that of the probe.

Front-face TR: The pump and probe are incident from the perovskite–air interface. The reflected probe from the perovskite–air interface is collected by the detector. The pump incident angle is near normal, and the probe incident angle is 45°.

Back-side transient reflection (BTR): The probe beams are incident on the sample from the perovskite–air interface, and the pump beam is shot on perovskite film from the substrate side. The reflected probe from the perovskite–air interface is collected by the detector. The pump incident angle is near normal, and the probe incident angle is 45°.

3. Results and Discussion

In this work, thin films of $(DMAPA)PbI_4$, a 2D D-J perovskite, are fabricated by the spin-coating method. Their thickness was measured by a cross section scanning electron microscopy (SEM), as shown in Fig. 1.

TA measurement is carried out on a 286 nm thick film. The pump wavelength is at 400 nm (above bandgap), and the pumping energy density is at 210 $\mu J/cm^2$ per pulse. Figure 2(b) shows a 2D contour plot of TA spectra, where the x axis is wavelength,

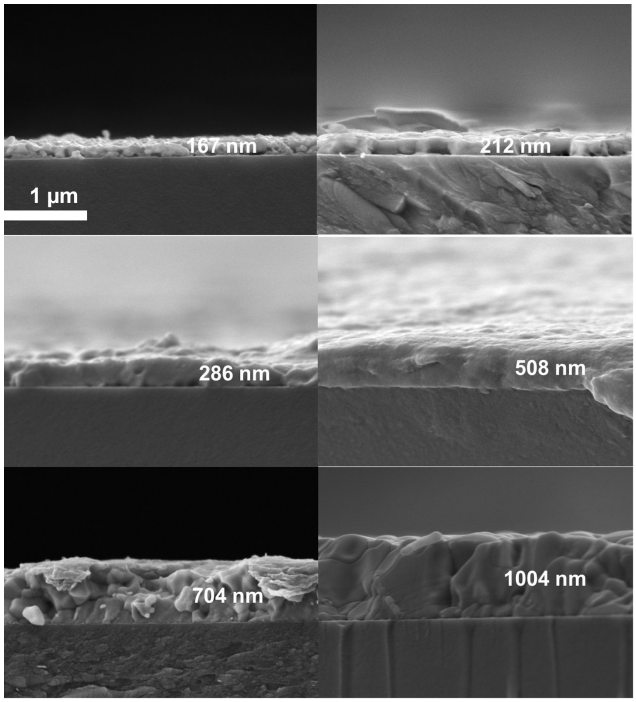

Fig. 1. Cross-sectional SEM images of the $(DMAPA)PbI_4$ films.

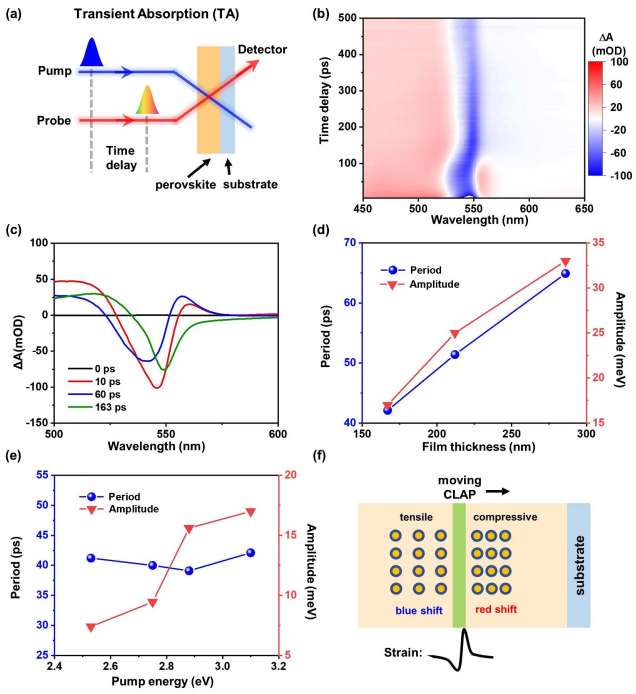

Fig. 2. (a) Scheme of TA experiments; (b) 2D contour plot of TA spectra; (c) ΔA spectra at selected time delays; (d) dependence of oscillation period and amplitude on film thickness; (e) dependence of oscillation period and amplitude on pump photon energy; (f) elucidating the origin of TA bandgap oscillation.

the y axis is delay time, and color denotes ΔA. Large spectral oscillation is observed. Figure 2(c) displays the TA spectra at different delay times. Initially, after excitation, a bleach peak centering at 546 nm is observed, with two positive "shoulders" caused by photoinduced absorption[22]. After that, the bleach peak redshifts to 541 nm at 60.5 ps and then blueshifts to 549 nm at around 163 ps. The shift of bleach peak indicates the bandgap of the perovskite film is oscillating for an amplitude of 33 meV.

Previous reports show that bandgap oscillation observed in TA spectra of perovskites could be the result of many factors, such as coherent optical phonons and optical Stark effect. Laser pulses induce coherent lattice displacement and vibration, known as coherent optical phonons, and some vibrational modes will modulate the bandgap. The bandgap oscillation period is correlated to vibration frequency, which is on the order of femtoseconds to picoseconds[17]. The optical Stark effect is a coherent interaction between the light field itself and matter[24]. Therefore, the time scale of Stark-induced bandgap oscillation will not be longer than the bandwidth of laser pulses, which is tens to hundreds of femtoseconds. The period of bandgap oscillation in Fig. 1(a) is around tens to hundreds of picoseconds. It cannot be explained by optical phonons and the optical Stark effect.

To elucidate the bandgap oscillation mechanism observed in this work, we perform TA experiments on films with different thicknesses, using different pump wavelengths. The dependence of the oscillation on the pump wavelength and film thickness is shown in Figs. 2(d) and 2(e), respectively. Increasing the pump photon energy makes the oscillation amplitude stronger, indicating that the oscillation is induced by the excess energy of pump photon (2.53–3.10 eV) relative to (DMAPA)PbI_4 bandgap (2.27 eV). The oscillation period has a positive correlation with film thickness, suggesting that the bandgap shift may be relevant to something longitudinally passing through the perovskite film. We also studied the effect of varied pump beam fluence on the same film. A positive correlation is also observed between oscillation amplitude and the pump fluence, while the oscillation period remains constant. Based on these dependencies, we hypothesize that the oscillation originates from the cross-plane transport of CLAPs.

When the energy of the absorbed photon is higher than the bandgap, hot electron–hole pairs are generated. As hot excitons quickly cool down, excess energy is transferred to the perovskite lattice through electron–phonon coupling, generating a transient stress at the incident surface. This stress results in a strain wave (CLAP), which propagates from the surface into the deeper sample at the sound speed[25,26].

Figure 2(f) elucidates why the CLAP causes an oscillation in TA measurement. The CLAP contains a tensile strain at the wavefront and a compressive region behind; they are separated by the center of the CLAP[27]. The strain modifies the bandgap of the perovskite that it influences. The bleach peak is redshifted when the lattice is compressed, or blueshifted when the lattice is stretched[28]. As the CLAP bounces back and forth between the surfaces, the fraction of stretched/compressed regions alters. Considering that the TA is the averaged result of the photoinduced changes through the entire sample, a blueshift and a redshift of TA spectra are observed.

In the TA spectra, only one swing in bandgap is observed instead of periodic oscillations, indicating that the CLAP only bounces once on the substrate–perovskite interface. That is caused by the low reflectivity of the CLAP on the interface of perovskites and glass, which we used as the substrate. The reflection coefficient (α_{re}) of the phonon of the perovskite–glass interface calculated by the acoustic mismatch model[29] is as small as 0.053, indicating that glass–perovskite interface is incapable of reflecting phonons. If the substrate is made by sapphire, which has a stronger phonon reflectivity ($\alpha_{re} = 0.42$), more periods of oscillations in the TA spectra may be observed[25].

To verify the presence of the CLAP, a front-face TR experiment is performed using 400 nm pump beam. A 2D color map is shown in Fig. 3(b), where the color represents $\Delta R/R$ this time. $\Delta R/R$ is proportional to the change in refractive index (Δn) of perovskite caused by the pump beam at the air interface. A pair of antisymmetric peaks is observed around the band edge, according to Kramers–Kronig relationship; the inverse Hilbert transform of Δn is proportional to ΔA, and therefore, this pair of peaks is relevant to bandgap bleach in the TA experiments. A set of sharp oscillations over wavelengths between 550 and 800 nm stem from the interference of probe light reflected from the front side and back side of the sample film[30].

In Fig. 3(b), an oscillation over time can also be observed. $\Delta R(t)/R(t)$ at different wavelengths are shown in Fig. 3(c). This figure shows that the oscillation periods at different wavelengths

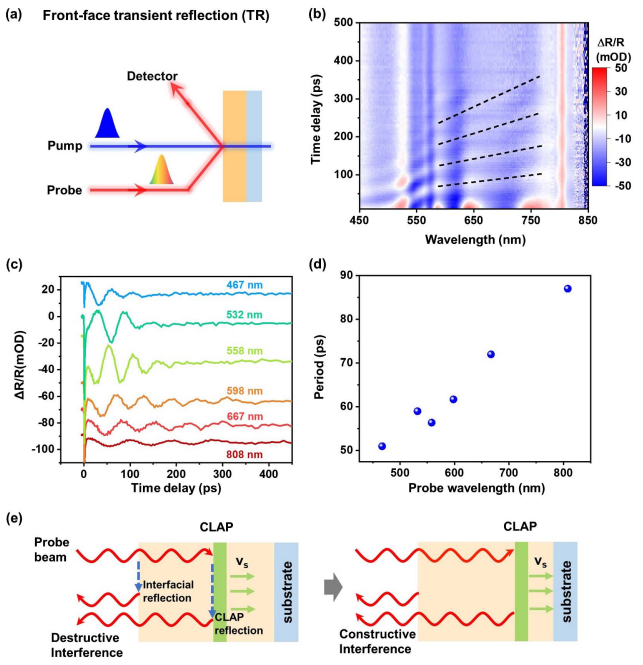

Fig. 3. (a) Scheme of front-face TR experiments; (b) 2D contour plot of TR spectra; (c) time-dependent $\Delta R/R$ at selected wavelengths; (d) dependence of oscillation period on wavelength of probe light; (e) elucidating the origin of oscillation observed in TR experiments.

are different. The periods are calculated by a fast Fourier transform (FFT) and plotted in Fig. 3(d). The oscillation period was positively correlated with the probe wavelength, confirming the cross-plane ballistic transportation of CLAPs[31].

Figure 3(e) explains this time-dependent oscillation. The CLAP itself is a discontinuity of the refractive index; therefore it can reflect the probe beam. The probe light reflected by the CLAP interferes with those reflected at the perovskite–air interface. As the CLAP is propagating into the sample at sound velocity, the interfering distance is changed, leading to the oscillation in probe intensity. The oscillation period T can be computed by the following equation[27]:

$$T = \frac{\lambda}{2nV_s \cos\theta},$$

where λ is the probe wavelength, n is the refractive index at the corresponding wavelength, V_s is the sound velocity, and θ is the probe light incidence angle. The equation predicts longer oscillation periods at longer probe wavelengths, which agrees well with the observation. The only exception is that longer oscillation is observed at 532 nm than at 558 nm, which is explained by the change in refractive index around the band edge.

To gain a deeper insight into the influence of the CLAP, BTR measurement is performed under a 400 nm pump. Figure 4(b) shows the 2D contour plot of BTR spectra of a 704 nm-thick $(DMAPA)PbI_4$ film. The difference between the BTR and the TR is that the pump beam is incident from the substrate side.

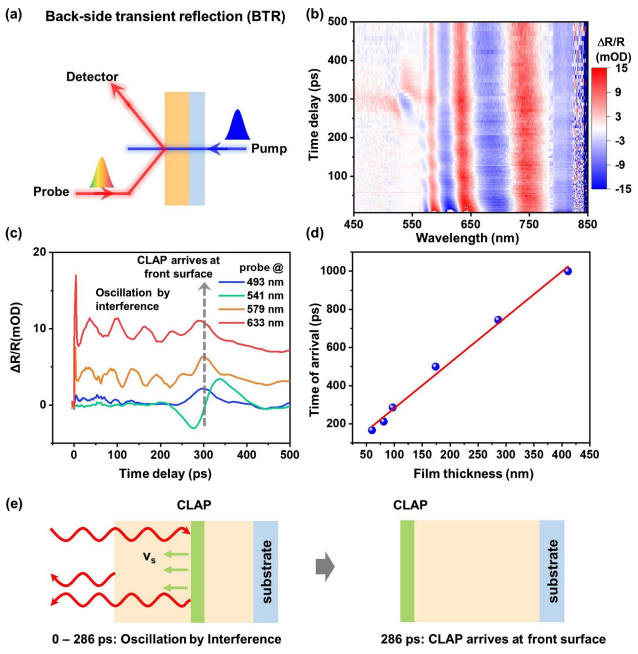

Fig. 4. (a) Scheme of BTR experiments; (b) 2D contour plot of BTR spectra; (c) time-dependent $\Delta R/R$ at selected wavelengths; (d) time when the CLAP arrives at air–perovskite interfaces for films of different thicknesses; (e) elucidating the origin of oscillation, and the CLAP arrival time observed in BTR experiments.

So, the sample is pumped and probed at different sides. Oscillation over wavelength is also observed in BTR due to the interference at the front and back surfaces.

In Fig. 4(c), which plots the time evolution of $\Delta R/R$ at different wavelengths, the oscillation over time between 0 and 300 ps is also caused by the interference of the probe beam reflected at the perovskite–air interface and by the CLAP, the same mechanism as in TR. Besides that, a "bump" in $\Delta R/R$ can be seen at the same delay time across all probe wavelengths. This is attributed to the arrival of the CLAP at the front surface.

The arrival time should be correlated to film thickness, so we performed BTR measurement on samples with different thicknesses. The CLAP arrival time in films at different thicknesses is shown in Fig. 4(d). A linear correlation is displayed, indicating that the CLAP transports ballistically inside the perovskite film. The slope of the curve, 2386 m/s, is the sound velocity in the film. This number is larger than the sound velocity in typical 2D R-P perovskites[32], indicating more efficient transport of acoustic phonons in the lattice of the D-J phase.

We also attempt to look for CLAPs in 3D ($MAPbI_3$) and R-P phase 2D perovskites. TR experiments show that CLAPs can be generated by optical excitation in these materials[32]. However, no or very small bandgap oscillations are observed in the TA experiments. That suggests a strong coupling between excited charge carriers and the lead–halide framework, and long modulation of strain on the bandgap in the D-J phase perovskites. In D-J phase perovskites, the two cations that separate the adjacent organic layers are connected by a covalent bond instead of van der Waals interactions, resulting in a larger elastic modulus in cross-plane direction compared to the R-P phase[16]. Therefore, a larger stress could be generated by the same amount of extra pump energy[25], leading to a stronger bandgap modulation. For the same reason, D-J phase perovskites exhibit longer coherence time of phonons[32]. Their large bandgap oscillation raises opportunities in ultrafast modulation of their bandgap energies and extension of absorbance spectra, improving the harvest of sunlight in their applications in solar cells.

4. Conclusions

In this work, we observe a strong and slow bandgap oscillation in the thin film of a 2D D-J phase perovskite, $(DMAPA)PbI_4$, in TA spectra after optical excitation. The oscillation correlates to a large bandgap shift up to 33 meV.

The oscillation has a dependence on the pump photon energy and film thickness, suggesting it originates from the transport of CLAPs across the film. When the energy in the excitation photon is larger than perovskite bandgap, excess energy is transferred into the lattice, generating acoustic phonons and a local strain. The strain propagates in the film by the speed of sound, modulating the bandgap of the lattice around it. As the CLAP moves, the ratio between compressed and stretched regions changes, making the spectra oscillate.

The presence of the CLAP is confirmed by the TR experiments. In front-face TR, spectral oscillation is also observed.

This oscillation is caused by the interference of the probe laser beam reflected at the air–perovskite interface and reflected by the CLAP. The motion of the CLAP changes the interference distance, leading to the spectral oscillation. In BTR, the arrival of the CLAP at the free surface was observed, and the sound velocity was calculated to be 2386 m/s with that information.

In 3D and 2D R-P phase perovskites, notable CLAP transport can only be observed in TR experiments. Large bandgap oscillation perovskites from the TA experiments indicate a stronger coupling between carriers and lattice and the larger effect of local strain on band energy in the D-J phase. This observation provides opportunities for future dynamical bandgap modulation in D-J phase perovskites.

Acknowledgement

This work was supported by the Ministry of Science and Technology (No. 2018YFA0208704) and the National Natural Science Foundation of China (No. 22173096).

References

1. D. Li, D. Zhang, K. S. Lim, Y. Hu, Y. Rong, A. Mei, N. G. Park, and H. Han, "A review on scaling up perovskite solar cells," Adv. Funct. Mater. **31**, 2008621 (2020).
2. R. Azmi, E. Ugur, A. Seitkhan, F. Aljamaan, A. S. Subbiah, J. Liu, G. T. Harrison, M. I. Nugraha, M. K. Eswaran, and M. J. S. Babics, "Damp heat–stable perovskite solar cells with tailored-dimensionality 2D/3D heterojunctions," Science **376**, 73 (2022).
3. H. Zhu, Y. Ren, L. Pan, O. Ouellette, F. T. Eickemeyer, Y. Wu, X. Li, S. Wang, H. Liu, X. Dong, S. M. Zakeeruddin, Y. Liu, A. Hagfeldt, and M. Gratzel, "Synergistic effect of fluorinated passivator and hole transport dopant enables stable perovskite solar cells with an efficiency near 24," J. Am. Chem. Soc. **143**, 3231 (2021).
4. Y. Yin, W. Tian, H. Luo, Y. Gao, T. Zhao, C. Zhao, J. Leng, Q. Sun, J. Tang, P. Wang, Q. Li, X. Lü, J. Bian, and S. Jin, "Excellent carrier transport property of hybrid perovskites sustained under high pressures," ACS Energy Lett. **7**, 154 (2021).
5. L. N. Quan, M. Yuan, R. Comin, O. Voznyy, E. M. Beauregard, S. Hoogland, A. Buin, A. R. Kirmani, K. Zhao, A. Amassian, D. H. Kim, and E. H. Sargent, "Ligand-stabilized reduced-dimensionality perovskites," J. Am. Chem. Soc. **138**, 2649 (2016).
6. Q. Sun, C. Zhao, Z. Yin, S. Wang, J. Leng, W. Tian, and S. Jin, "Ultrafast and high-yield polaronic exciton dissociation in two-dimensional perovskites," J. Am. Chem. Soc. **143**, 19128 (2021).
7. W. Tao, Y. Zhang, and H. Zhu, "Dynamic exciton polaron in two-dimensional lead halide perovskites and implications for optoelectronic applications," Acc. Chem. Res. **55**, 345 (2022).
8. G. Wu, R. Liang, M. Ge, G. Sun, Y. Zhang, and G. Xing, "Surface passivation using 2D perovskites toward efficient and stable perovskite solar cells," Adv. Mater. **34**, 2105635 (2022).
9. X. Zhao, T. Liu, and Y. L. Loo, "Advancing 2D perovskites for efficient and stable solar cells: challenges and opportunities," Adv. Mater. **34**, 2105849 (2022).
10. J. Tang, W. Tian, C. Zhao, Q. Sun, C. Zhang, H. Cheng, Y. Shi, and S. Jin, "Imaging the moisture-induced degradation process of 2D organolead halide perovskites," ACS Omega **7**, 10365 (2022).
11. C. Katan, N. Mercier, and J. Even, "Quantum and dielectric confinement effects in lower-dimensional hybrid perovskite semiconductors," Chem. Rev. **119**, 3140 (2019).
12. C. M. Mauck and W. A. Tisdale, "Excitons in 2D organic–inorganic halide perovskites," Trends Chem. **1**, 380 (2019).
13. J. C. Blancon, J. Even, C. C. Stoumpos, M. G. Kanatzidis, and A. D. Mohite, "Semiconductor physics of organic-inorganic 2D halide perovskites," Nat. Nanotechnol. **15**, 969 (2020).
14. L. Mao, W. Ke, L. Pedesseau, Y. Wu, C. Katan, J. Even, M. R. Wasielewski, C. C. Stoumpos, and M. G. Kanatzidis, "Hybrid Dion-Jacobson 2D lead iodide perovskites," J. Am. Chem. Soc. **140**, 3775 (2018).
15. P. Fu, Y. Liu, S. Yu, H. Yin, B. Yang, S. Ahmad, X. Guo, and C. Li, "Dion-Jacobson and Ruddlesden-Popper double-phase 2D perovskites for solar cells," Nano Energy **88**, 106249 (2021).
16. J. Gong, M. Hao, Y. Zhang, M. Liu, and Y. Zhou, "Layered 2D halide perovskites beyond the Ruddlesden–Popper phase: tailored interlayer chemistries for high-performance solar cells," Angew. Chem. Int. Ed. **61**, e202112022 (2022).
17. P. Guo, Y. Xia, J. Gong, D. H. Cao, X. Li, X. Li, Q. Zhang, C. C. Stoumpos, M. S. Kirschner, H. Wen, V. B. Prakapenka, J. B. Ketterson, A. B. F. Martinson, T. Xu, M. G. Kanatzidis, M. K. Y. Chan, and R. D. Schaller, "Direct observation of band gap oscillations induced by optical phonons in hybrid lead iodide perovskites," Adv. Funct. Mater. **30**, 1907982 (2020).
18. H. Kim, J. Hunger, E. Canovas, M. Karakus, Z. Mics, M. Grechko, D. Turchinovich, S. H. Parekh, and M. Bonn, "Direct observation of mode-specific phonon-band gap coupling in methylammonium lead halide perovskites," Nat. Commun. **8**, 687 (2017).
19. Y. Li, S. He, X. Luo, X. Lu, and K. Wu, "Strong spin-selective optical Stark effect in lead halide perovskite quantum dots," J. Phys. Chem. Lett. **11**, 3594 (2020).
20. Y. Yang, M. Yang, K. Zhu, J. C. Johnson, J. J. Berry, J. van de Lagemaat, and M. C. Beard, "Large polarization-dependent exciton optical Stark effect in lead iodide perovskites," Nat. Commun. **7**, 12613 (2016).
21. D. Giovanni, W. K. Chong, H. A. Dewi, K. Thirumal, I. Neogi, R. Ramesh, S. Mhaisalkar, N. Mathews, and T. C. Sum, "Tunable room-temperature spin-selective optical Stark effect in solution-processed layered halide perovskites," Sci. Adv. **2**, e1600477 (2016).
22. W. Zhao, Q. Dong, J. Zhang, S. Wang, M. Chen, C. Zhao, M. Hu, S. Jin, N. P. Padture, and Y. Shi, "Asymmetric alkyl diamine based Dion–Jacobson low-dimensional perovskite solar cells with efficiency exceeding 15%," J. Mater. Chem. A **8**, 9919 (2020).
23. J. Liu, J. Leng, K. Wu, J. Zhang, and S. Jin, "Observation of internal photoinduced electron and hole separation in hybrid two-dimensional perovskite films," J. Am. Chem. Soc. **139**, 1432 (2017).
24. S. H. Autler and C. H. Townes, "Stark effect in rapidly varying fields," Phys. Rev. **100**, 703 (1955).
25. C. Thomsen, J. Strait, Z. Vardeny, H. J. Maris, J. Tauc, and J. J. Hauser, "Coherent phonon generation and detection by picosecond light pulses," Phys. Rev. Lett. **53**, 989 (1984).
26. P. Ruello and V. E. Gusev, "Physical mechanisms of coherent acoustic phonons generation by ultrafast laser action," Ultrasonics **56**, 21 (2015).
27. C. Thomsen, H. T. Grahn, H. J. Maris, and J. Tauc, "Surface generation and detection of phonons by picosecond light pulses," Phys. Rev. B **34**, 4129 (1986).
28. D. Liu, D. Luo, A. N. Iqbal, K. W. P. Orr, T. A. S. Doherty, Z. H. Lu, S. D. Stranks, and W. Zhang, "Strain analysis and engineering in halide perovskite photovoltaics," Nat. Mater. **20**, 1337 (2021).
29. E. T. Swartz and R. O. Pohl, "Thermal boundary resistance," Rev. Mod. Phys. **61**, 605 (1989).
30. Y. Yang, M. Yang, D. T. Moore, Y. Yan, E. M. Miller, K. Zhu, and M. C. Beard, "Top and bottom surfaces limit carrier lifetime in lead iodide perovskite films," Nat. Energy **2**, 16207 (2017).
31. J. K. Miller, J. Qi, Y. Xu, Y. J. Cho, X. Liu, J. K. Furdyna, I. Perakis, T. V. Shahbazyan, and N. Tolk, "Near-band gap wavelength dependence of long-lived traveling coherent longitudinal acoustic phonons in GaSb-GaAs heterostructures," Phys. Rev. B **74**, 113313 (2006).
32. P. Guo, C. C. Stoumpos, L. Mao, S. Sadasivam, J. B. Ketterson, P. Darancet, M. G. Kanatzidis, and R. D. Schaller, "Cross-plane coherent acoustic phonons in two-dimensional organic-inorganic hybrid perovskites," Nat. Commun. **9**, 2019 (2018).